



Photocatalytic degradation of several VOCs (*n*-hexane, *n*-butyl acetate and toluene) on TiO₂ layer in a closed-loop reactor

František Moulis*, Josef Krýsa**

Institute of Chemical Technology, Prague, Technická 5, 166 28 Prague 6, Czech Republic

ARTICLE INFO

Article history:

Received 26 June 2012

Received in revised form 3 October 2012

Accepted 16 October 2012

Available online 3 December 2012

Keywords:

Photocatalysis

Gas-phase

n-Hexane

n-Butyl acetate

Toluene

Closed loop

ABSTRACT

This paper deals with photocatalytic degradation of three VOCs differing in chemical structure (*n*-hexane, *n*-butyl acetate and toluene) in a closed-loop reactor. Degradation tests were performed on particulate layers prepared from TiO₂ VLP7000 (Kronos). Concentration dependencies of VOCs were simulated and initial degradation rates calculated. Dependence of the latter on initial concentrations confirms single-site Langmuir–Hinshelwood kinetics with value of hexane adsorption constant 0.023 m³ mmol⁻¹. It was shown that butyl acetate is oxidized preferably to hexane when they react in a mixture, while their individual degradation seems to be kinetically similar. Toluene deactivates the photocatalyst and its degradation is thus very slow but the catalyst can be renewed by thermal treatment. The found selectivity or inhibitive ability of investigated VOCs in mixture is important for the proper choice of a suitable purification method of industrial exhaust fumes.

© 2012 Elsevier B.V. All rights reserved.

1. Introduction

Harmful agents, e.g. volatile organic compounds (VOCs), are liberated into the environment [1] during a large range of industrial applications. There are two main domains of photocatalytic applications depending on the degree of air pollution: high-polluted gas from industrial processes (agents in concentrations in order of hundreds ppm) and low-contaminated air (order of units ppm). Several conventional methods for VOC removal from industrial exhausts exist differing in concentrations they can be applied on, removal efficiency, costs, secondary risks or some other restraints [2]. Thermal oxidation, catalytic oxidation, carbon adsorption or absorption in a liquid solvent allow removal efficiency 90–99%, condensation is less effective (50–90%). All these methods produce secondary waste in the form of combustion products, spent carbon, wastewater or condensate, which must be treated subsequently.

From the industrial point of view, carbon adsorption can handle VOC concentrations from 20 to 5000 ppm and can be combined with VOC recover; the organic solvent is commonly released by heating the carbon with steam and then separated by means of decantation or distillation [3]. Besides the techniques mentioned above, biological treatment can be used alternatively at low VOC

concentrations (μg/m³, order of ppb). However, this technique brings numerous challenges as well, e.g. the maintenance of microbial growth in the polluted medium [4]. Comparing photocatalytic degradation to contemporary (conventional) processes, the former leads to the decomposition of pollutant towards non-harmful compounds in one step at ambient conditions; no secondary waste is produced. This makes from photocatalytic process a method with good performance [5], especially at low concentrations [6–8].

In industrial domain of application, only continuous reactors seem to be efficient regarding the large flow rates treated [9,10]. However, in this paper we describe a batch (closed-loop) reactor, which is more convenient for the evaluation of photocatalyst.

Heterogeneous photocatalytic reaction occurs in the presence of photon at sufficient energy (wavelength), catalytic surface and oxidizing agent (mostly molecular oxygen). The photon energy must be higher than the photocatalyst band-gap one. Photocatalyst surface excitation leads to the formation of free electrons in the conductivity band and positively charged holes in the valence band. These electron–hole pairs are then used in oxidative mechanisms to form hydroxyl radicals (from water) and superoxide ions (from oxygen). Besides these reactions reverse recombination of electron–hole pairs exists and is the main limiting factor that lowers the efficiency of photocatalytic processes [11].

Already in 1964 McIntock and Ritchie showed that organic compounds ethylene and propylene can be completely oxidized to CO₂ and H₂O [12]. Today, comparing the number of scientific publications to the number of patents dealing with photocatalysis, the majority of scientific publications deals with the degradation in

* Corresponding author. Tel.: +420 220 444 390; fax: +420 220 444 410.

** Corresponding author. Tel.: +420 220 444 112; fax: +420 220 444 410.

E-mail addresses: frantisek.moulis@vscht.cz, moulisf@vscht.cz (F. Moulis), josef.krýsa@vscht.cz (J. Krýsa).

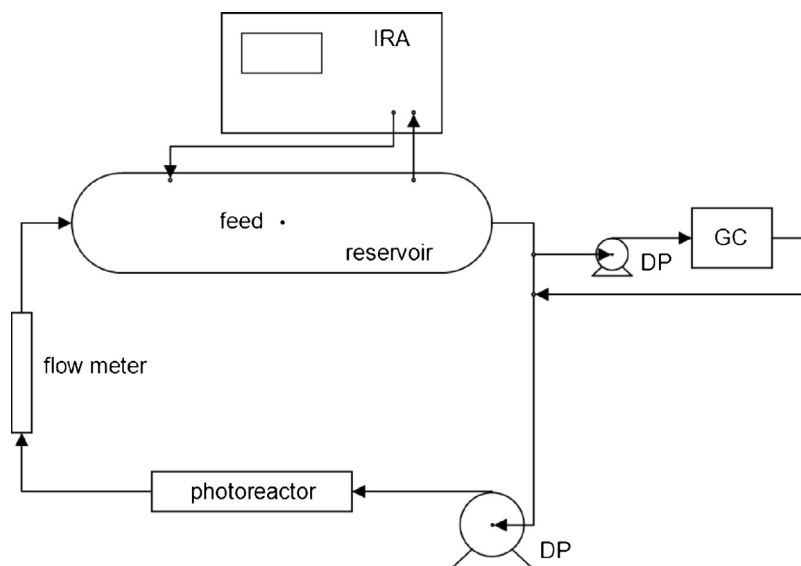
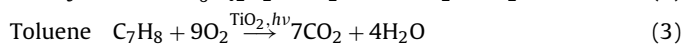
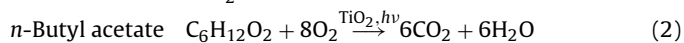


Fig. 1. Apparatus scheme. IRA – mobile infrared analyser; DP – diaphragm pump.

water phase, while the patents are focused rather on the gaseous phase [13]. This suggests that the application potential of photocatalysis is in the air purification domain. The real scientific interest in photocatalysis in gaseous phase started in 1990s [14–18] and the number of publications has grown sharply since 1995 [13].

This paper deals with some aspects of photocatalytic degradation of several model VOCs (*n*-hexane [19–22], *n*-butyl acetate [23] and toluene [5,7,10,18,20,24–32]) in a closed-loop reactor. These pollutants were chosen for their different chemical structure, which results in different chemical properties, e.g. water solubility; these are also abundantly used as industrial solvents. For instance, they occur in automotive industry, namely in the process of plastics treatment, where aromates, alkenes, alkyl esters or some other hydrocarbons coexist. Their photocatalytic mineralization can be summarized by overall chemical reactions (1)–(3).



The mentioned compounds were studied separately but also at operational conditions similar to industrial exhaust fumes as degradation in a mixture and subsequent pollutant injection.

2. Experimental

2.1. Apparatus

The apparatus has recirculation loop geometry. It is composed of diaphragm pump AL-6SB (Alita, Slovak Republic), photoreactor and reservoir (in direction of circulation). Infrared analyser and gas chromatograph are connected in parallel. Tubing is made of polyamide tubes and push-in fittings. Apparatus volume is 2.85 dm³. The recirculation rate is held constant at value about 0.2 Nm³/h. The scheme of the entire apparatus is shown in Fig. 1.

The photoreactor is designed as a plate reactor, i.e. that the air flows over the 15 by 18 cm photoactive layer in a thin film. The air enters the reactor from jets in its shorter side and flows through by an average velocity of ca. 5 cm s⁻¹. Three 11 W lamps Sylvania BLB with emission maximum at 367 nm were used as external UV sources; the average light intensity was 2 mW cm⁻².

The reaction mixture is initially composed only of air and the model pollutant(s). The air is taken directly from laboratory at

its ambient conditions; its initial relative humidity was measured ranging from 40 to 50%. The liquid pollutant is injected through the feed septum into the reservoir. A period of several minutes precedes the start of degradation experiment in order to evaporate the pollutant and to get a homogeneous mixture.

Concentration of individual pollutants and possible intermediates was determined by gas chromatograph Varian CP-3800 with capillary column CP-Sil 5 CB 15 × 0.25 (0.25) and flame ionization detector. Mobile infrared analyser (Aseko, Czech Republic) is equipped with infrared gas cell and is calibrated for on-line measurement of CO₂ concentration, which enables the evaluation of overall mineralization rate. Intermediates adsorbed on the surface of photocatalyst were analysed directly with FT-IR spectrometer Nicolet iS10. Gas chromatography (column DB-5MS 60 m × 0.32 mm × 1 μm) with mass detection was used for analysis of desorbed species; this was done by headspace method, i.e. the catalyst was heated for 15 min at 150 °C and the desorbed gases were analysed.

2.2. Particulate layer preparation

Particulate layers were prepared from TiO₂ water suspension; the suspension was placed on the substrate and was left to dry out, then was thermally treated at 300 °C. Glass sheets of dimensions 15 cm × 18 cm were used as a support. Amount of TiO₂ was 0.5 mg cm⁻², used TiO₂ photocatalyst VLP7000 (Kronos). This photocatalyst was selected on the base of a previous study comparing photoactivity of four different TiO₂ photocatalysts in gaseous phase (L.A. García, Diploma thesis: Photocatalytic degradation of pollutants in liquid and gaseous phase, ICT Prague, 2010). For instance, we give a comparison to standard P25 material in Fig. 2, from which is seen that the degradation is faster on VLP7000 and this is confirmed by faster generation of CO₂. Some characteristics for both materials are listed in Table 1, from which it can be seen that VLP7000

Table 1
Material characteristics of photocatalysts.

Material (producer)	Specific surface (m ² g ⁻¹)	Crystal size (nm)	Crystalline structure
VLP7000 (Kronos)	267	7	Anatase
P25 (Degussa)	56	Anatase 22 Rutile 41	Anatase 71% Rutile 29%

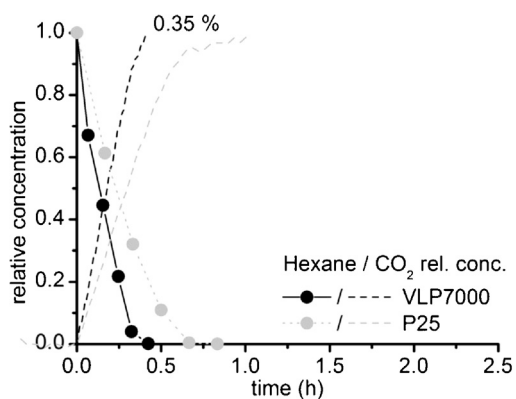


Fig. 2. Hexane degradation on VLP7000 compared to P25 at initial concentration 830 ppm; data normalized by the maximal concentration.

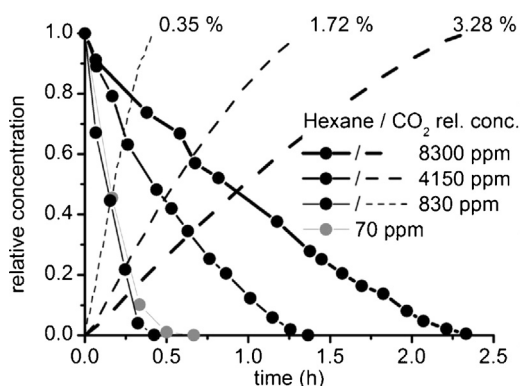


Fig. 3. Hexane degradation at different initial concentrations; final volume concentrations of CO₂ are indicated at the end of each curve.

has several times higher specific surface and in contrast to P25 is composed of pure anatase.

3. Results and discussion

3.1. Influence of the initial concentration

The influence of initial hexane concentration was studied at values of 70, 830, 4150 and 8300 ppm (2.9, 34.3, 171.4 and 342.7 mmol m⁻³ at 22 °C). The progress of all four experiments is shown in Fig. 3 in relative concentrations of hexane. The lower the initial concentration, the lower the time necessary for complete pollutant degradation. Relative concentrations of CO₂ (related to the final concentrations) are also shown in Fig. 3, only for the lowest initial concentration of hexane, signal of CO₂ was not detectable. It can be seen that for an order higher initial concentration of hexane (8300 ppm) we reach an order higher CO₂ concentration (3.28%).

Photocatalytic experiments in the gaseous phase are performed rather in continuous reactors [5,6,9,10,14,15,17–25,28,30–34] than in closed-loop (batch) reactors [16,26,27,29,35,36]. These two configurations have some important differences from the kinetic point of view. Firstly, the intermediates have not such importance in continuous systems than in the batch ones, where they can easily accumulate and thus make a kinetic study more difficult. Secondly, the determination of degradation rate seems to be easier in the continuous systems where a conversion can be used almost directly. On the other hand, this cannot be done for batch systems, where time dependence must be taken into account and analysed; an initial degradation rate must be defined somehow or parameters of an appropriate kinetic model must be determined.

In most cases the pollutant photocatalytic destruction on the TiO₂ is assumed to follow single-site Langmuir–Hinshelwood (L–H) kinetics [34]. The reaction rate $r(0)$ is defined as (in mol s⁻¹):

$$r(0) = k_{LH} \frac{K_L c(0)}{1 + K_L c(0)} \quad (4)$$

where k_{LH} is the apparent L–H rate constant in mol s⁻¹, K_L the Langmuir adsorption constant in m³ mol⁻¹ and $c(0)$ is the initial concentration in mol m⁻³. Mathematic fit using the form of Eq. (4) was done for C₅–C₇ hydrocarbons degradation in gaseous phase [19]. In that case instantaneous concentrations in a continuous (flow-through) system were used and L–H kinetics was justified by low initial concentrations (40–130 ppm) and thus negligible by-products concentrations. L–H model was used also for ethanol degradation and its intermediates (acetaldehyde, formaldehyde) and transient model was established [35]. Determination of L–H parameters was calculated from initial rates and initial concentrations issued from several experiments. As the experiment was carried out in a closed recirculation loop, the complete mineralization was followed as well. For general photodegradation experiment in a closed-loop system, the single-site L–H model [Eq. (4)] is valid only for the initial concentration, thus only for the initial reaction rate when the by-products are produced in a negligible amount. For this purpose, we define initial degradation rate R_i (mmol m⁻² h⁻¹) by Eq. (5):

$$R_i = \frac{n_0}{A} \left(\frac{dc_{rel}}{dt} \right)_i \quad (5)$$

where n_0 is the initial molar amount of pollutant, A the irradiated area, c_{rel} the relative pollutant concentration [actual concentration $c(t)$ divided by the initial one $c(0)$, i.e. $c_{rel} = c(t)/c(0)$], t the time, $(dc_{rel}/dt)_i$ is the initial slope of concentration dependence on irradiation time. As a first step we need to fit the experimental data by suitable function and then calculate initial slope of this function.

Fig. 4a–c shows some possibilities how to fit experimental data from a degradation experiment in closed-loop photoreactor. Exponential fit (assumption of first order kinetics) shows deviations for short and also long irradiation times. Linear fit applied on several first points is represented as well; however, the problem is how

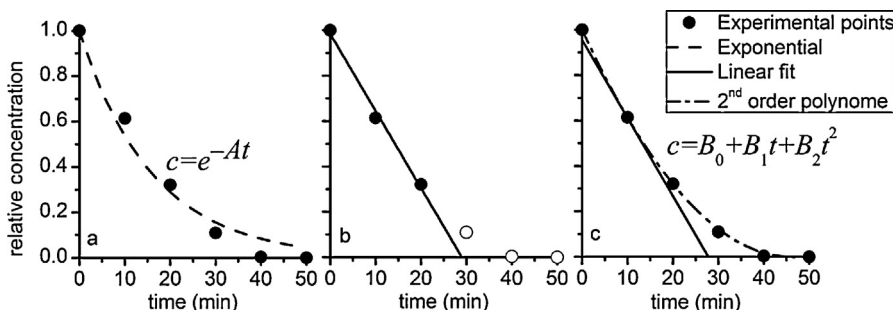


Fig. 4. Exponential, linear and polynomial fit of a general degradation experiment; points used for the fit are represented by solid circles.

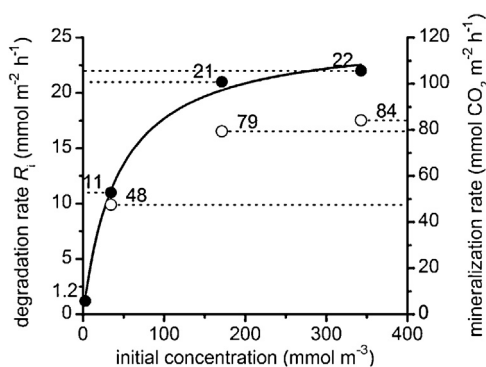


Fig. 5. Dependence of initial degradation rate of hexane on initial concentration, fit done by Eq. (6); initial mineralization rate is also indicated.

many points are taken into account. As seen from Fig. 4c, a polynomial fit of 2nd order represents the concentration decay very accurately. To calculate the initial slope $(dc_{rel}/dt)_i$ we have chosen a sufficiently low fixed time $t=9$ min, so thus degradation rate R_i defined by Eq. (5) can be considered as the initial one.

Initial degradation rates calculated from the experimental data (Fig. 3) are shown in Fig. 5 as a dependence on the initial concentration; the data are fitted by Eq. (6):

$$R_i = 25.4 \frac{0.0228c(0)}{1 + 0.0228c(0)} \quad (6)$$

which compared to Eq. (4) would result in L–H parameters $k_{LH}=25 \text{ mmol m}^{-2} \text{ h}^{-1}$ and $K_L=0.023 \text{ m}^3 \text{ mmol}^{-1}$. As the kinetic constant k_{LH} is related to the immobilized catalyst surface, no further normalization is needed; this would be necessary e.g. for aqueous suspension of TiO_2 [37]. A significant change of reaction order follows from Fig. 5. We get first-order kinetics at low concentrations and zero-order kinetics at high concentrations. This change of order was already reported in gaseous phase for heptane [36], butyric acid [33] or some other alkanes [19].

The mineralization rate is calculated from the initial slope of CO_2 generation in Fig. 3, Eq. (1), known apparatus volume and equation of state for ideal gas. The results are represented in Fig. 5 and are in good agreement with the initial degradation rates. Carbon balance results in degree of mineralization around 0.7 for all three initial concentrations where CO_2 was measured.

Our parameters from Eq. (6) differ significantly from those reported previously for hexane degradation in continuous system ($k_{LH}=0.78 \text{ mmol m}^{-2} \text{ h}^{-1}$ and $K_L=13 \text{ m}^3 \text{ mmol}^{-1}$) [19]. Furthermore even in very reduced range of concentrations (up to 4 mmol m^{-3}) a zero-order region was reached already above concentration 1 mmol m^{-3} [19], which at our experimental conditions did not occur below 170 mmol m^{-3} (see Fig. 5). The main reason for the deviation could be different experimental conditions. Boulamanti [19] used continuous system, different UV light wavelength (254 nm) and different photocatalyst with higher coverage (P25 , 3.5 mg cm^{-2}), UV light intensity was not reported. Zhang [22] investigated hexane degradation in a continuous system with a 254 nm UV lamp and got similar value of adsorption constant ($K_L=4.4 \text{ m}^3 \text{ mmol}^{-1}$) as Boulamanti [19].

We found adsorption constant K_L on TiO_2 for similar compound – *n*-heptane – as $0.31 \text{ m}^3 \text{ mmol}^{-1}$ issued from pure adsorption isotherm measurement [29] or as $0.030 \text{ m}^3 \text{ mmol}^{-1}$ issued from degradation experiments in batch reactor with UV light wavelength 365 nm [36]. Our value ($0.023 \text{ m}^3 \text{ mmol}^{-1}$) for hexane is in very good agreement with that for heptane ($0.030 \text{ m}^3 \text{ mmol}^{-1}$) [36]. It is most probably due to the similar experimental conditions: closed-loop photoreactor, wavelength (365 nm) and light intensity ($\sim 5 \text{ mW cm}^{-2}$). The smaller value of our K_L can be explained by

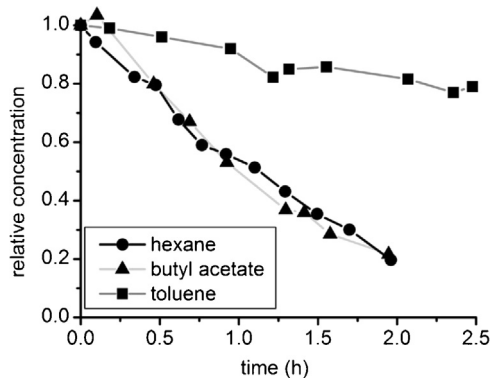


Fig. 6. Consecutive degradations of model pollutants at initial concentration 8300 ppm.

already reported decrease of K_L issued from a degradation experiment with increasing light intensity [33]. Our experiments thus show that crucial parameters influencing the value of adsorption constant K_L are light wavelength and experimental configurations (continuous versus closed-loop) arrangement.

3.2. Comparison of the model pollutants

Consecutive photocatalytic degradations of three air pollutants are compared in Fig. 6 in the order hexane, butyl acetate and toluene. The degradation kinetics of butyl acetate is similar to the hexane one but degradation rate of toluene is considerably lower. Furthermore, the photocatalyst changed the colour from white towards yellow brown after toluene degradation experiment. This deactivation was already reported for toluene concentrations higher than 13 ppm [20,24,26–28,30]. Stable activity of TiO_2 photocatalyst was observed at low toluene concentrations (35 ppb) [7] or with special polycrystalline TiO_2 (Merck) [31]. Using GC-MS we detected adsorbed species on the photocatalyst, e.g. benzoic acid, benzaldehyde and probably methylphenyl benzoate. Adsorption of benzaldehyde and benzoic acid on TiO_2 was reported to be irreversible [32]. Recently the presence of benzoate complexes on TiO_2 was confirmed by FT-IR [26]. In our case we observed bands at 1604, 1450 and 1415 cm^{-1} in the FT-IR spectrum which correspond to those in benzoate spectrum (1604 , 1454 and 1419 cm^{-1}) [26]. The only intermediate in the gaseous phase detectable by GC-FID was benzaldehyde in very low concentrations hundred times lower than toluene. It can be thus concluded that the irreversible adsorption of benzoic acid and benzaldehyde is responsible for photocatalyst deactivation.

Toluene degradation influenced negatively consecutive degradations carried out on the same layer. This is shown in Fig. 6, which compares hexane degradation ability of VLP7000 material in the form of fresh photocatalyst, toluene deactivated one and regenerated one. Although the rates of butyl acetate and hexane degradation are very similar (see Fig. 6), the deactivation impact of toluene on the consecutive degradations is stronger in hexane case than in butyl acetate case. Without any treatment photocatalyst remains deactivated but after its regeneration by thermal treatment (for 2 h at 300°C) the degradation ability was completely renewed.

3.3. Degradation of mixture of pollutants

In real life, industrial exhausts contain more than one pollutant. Thus we studied how a mixture of model pollutants is degraded, especially considering the different elimination of constituent pollutants. The initial concentration was set to 4150 ppm for both

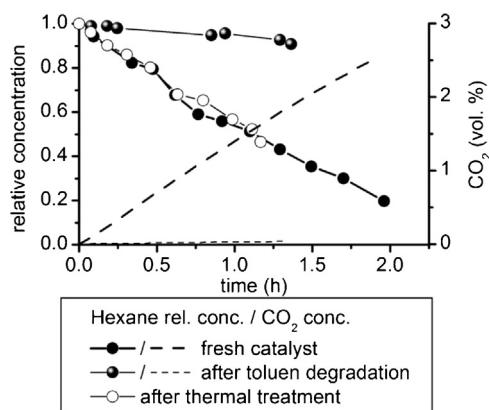


Fig. 7. Hexane degradation (8300 ppm) on the same layer before and after toluene degradation (8300 ppm).

pollutants in the binary mixture of hexane and butyl acetate (Fig. 8) in order to balance the photocatalyst utilization in the same manner as for the individual pollutants (8300 ppm; Fig. 6). There is an evident selectivity towards butyl acetate, which is degraded much faster as seen from Fig. 7. It takes approximately 2 h to eliminate the significant content of butyl acetate and to start the degradation of hexane in a more apparent way. The possible reason is the fifty times higher water solubility of butyl acetate (0.7% at 20 °C) than hexane (0.014% at 20 °C). Due to the presence of water microfilm on the photocatalyst surface [29], butyl acetate is easily adsorbed than hexane and thus easily degradable. As can be seen from the CO₂ concentration curve, the slope is fairly constant (it means very similar mineralization rate of both pollutants) and decreases significantly only when both pollutants are oxidized and thus not present in the system (3.75 h). The slope changes only slightly when all butyl acetate is degraded from the system (at about 2.5 h). This increase is consistent with higher mass of carbon in unit mass of hexane (comparing to butyl acetate) and with almost the same degradation rates of hexane and butyl acetate (Fig. 6).

Another possibility how to compare individual pollutants degradation in mixture is their progressive injection. This is represented in Fig. 9. Degradation of hexane (1 mmol, 8500 ppm) was interrupted by injecting butyl acetate (0.38 mmol, 3200 ppm). According to the supposition that butyl acetate is degraded preferentially (as in Fig. 6) the degradation of hexane was significantly slowed down in favour of the butyl acetate one. Nevertheless, CO₂ concentration grows nearly linearly with time and shows that the mineralization of both pollutants is uniform. However, toluene injection

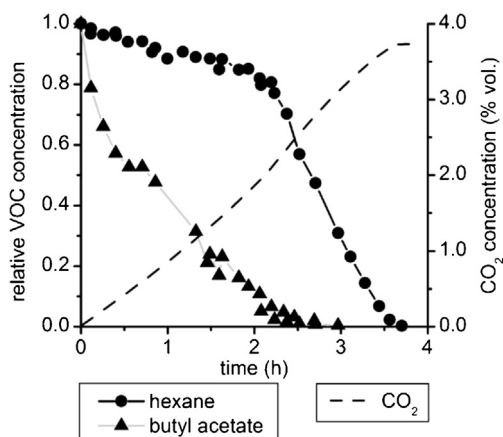


Fig. 8. Degradation of binary mixture of hexane and butyl acetate at initial concentrations 4150 ppm.

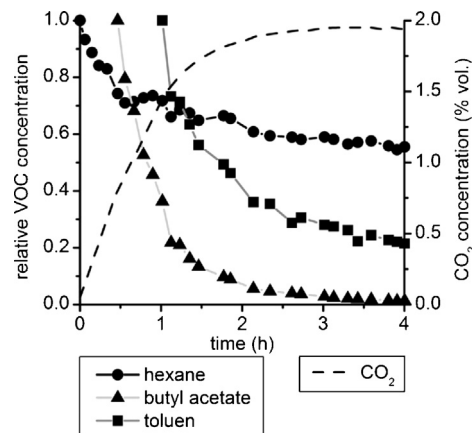


Fig. 9. Selective degradation of progressively injected pollutants: hexane (1 mmol, 8500 ppm), butyl acetate (0.38 mmol, 3200 ppm) and toluene (0.1 mmol, 860 ppm).

(0.1 mmol, 860 ppm) causes slowing down of butyl acetate degradation and also overall mineralization. Toluene itself is oxidized quickly immediately after injection but after about 1 h its degradation rate significantly decreases. Overall mineralization rate gradually decreases and after 3 h it is negligible as confirmed by the CO₂ concentration staying constant.

4. Conclusion

We have shown that hexane and butyl acetate can be photocatalytically degraded from air. Butyl acetate is oxidized preferably to hexane when they react in a mixture, while their individual degradation seems to be kinetically similar. Solubility of butyl acetate in water is about an order higher than that of hexane, which suggests that the oxidation reaction proceeds in the aqueous microfilm present on the surface of the TiO₂ photocatalyst. Dependence of initial degradation rates on initial concentration confirms single-site Langmuir–Hinshelwood kinetics with value of hexane adsorption constant 0.023 m³ mmol⁻¹.

Oxidation products of toluene deactivate the photocatalyst and its degradation is thus very slow at our operational conditions (TiO₂ photocatalyst VLP7000 and initial concentration 8300 ppm). We detected benzaldehyde, benzoic acid and methylphenyl benzoate as intermediates. The deactivation is fully reversible and the catalyst can be renewed by thermal treatment. The found selectivity or inhibitive ability of studied organic pollutants could play an important role in the purification of industrial exhaust fumes containing always more than one pollutant, e.g. can even block elimination of some pollutants if the preferentially degraded ones are present in an important concentration.

Acknowledgements

Authors acknowledge the financial support from the Ministry of Industry and Trade of the Czech Republic (project FR-TI3/242) and from specific university research (MSMT no. 21/2012). Authors would like also to thank Tomáš Floriš for his substantial contribution to the experimental part of the work.

References

- [1] J.J. Shah, H.B. Singh, *Environmental Science and Technology* 22 (1988) 1381–1388.
- [2] E.N. Ruddy, L.A. Carroll, *Chemical Engineering Progress* 89 (1993) 28–35.
- [3] M.J. Ruhl, *Chemical Engineering Progress* 89 (1993) 37–41.
- [4] B. Guieysse, C. Hort, V. Platel, R. Munoz, M. Ondarts, S. Revah, *Biotechnology Advances* 26 (2008) 398–410.

- [5] P. Pichat, J. Disdier, C. Hoang-Van, D. Mas, G. Goutailler, C. Gaysse, *Catalysis Today* 63 (2000) 363–369.
- [6] W.K. Jo, K.H. Park, *Chemosphere* 57 (2004) 555–565.
- [7] C.H. Ao, S.C. Lee, C.L. Mak, L.Y. Chan, *Applied Catalysis B: Environmental* 42 (2003) 119–129.
- [8] C.H. Ao, S.C. Lee, *Journal of Photochemistry and Photobiology A* 161 (2004) 131–140.
- [9] R. Portela, S. Suarez, R.F. Tessinari, M.D. Hernandez-Alonso, M.C. Canela, B. Sanchez, *Applied Catalysis B: Environmental* 105 (2011) 95–102.
- [10] A.J. Maira, J.M. Coronado, V. Augugliaro, K.L. Yeung, J.C. Conesa, J. Soria, *Journal of Catalysis* 202 (2001) 413–420.
- [11] A. Fujishima, X.T. Zhang, D.A. Tryk, *Surface Science Reports* 63 (2008) 515–582.
- [12] I.S. McIntoc, M. Ritchie, *Transactions of the Faraday Society* 61 (1965) 1007–1016.
- [13] Y. Paz, *Applied Catalysis B: Environmental* 99 (2010) 448–460.
- [14] L.A. Dibble, G.B. Raupp, *Environmental Science and Technology* 26 (1992) 492–495.
- [15] J. Peral, D.F. Ollis, *Journal of Catalysis* 136 (1992) 554–565.
- [16] L.A. Phillips, G.B. Raupp, *Journal of Molecular Catalysis* 77 (1992) 297–311.
- [17] G.B. Raupp, C.T. Junio, *Applied Surface Science* 72 (1993) 321–327.
- [18] T.N. Obee, R.T. Brown, *Environmental Science and Technology* 29 (1995) 1223–1231.
- [19] A.K. Boulamanti, C.J. Philippopoulos, *Atmospheric Environment* 43 (2009) 3168–3174.
- [20] O. d’Hennezel, D.F. Ollis, *Journal of Catalysis* 167 (1997) 118–126.
- [21] C.T. Brigden, S. Poulston, M.V. Twigg, A.P. Walker, A.J.J. Wilkins, *Applied Catalysis B: Environmental* 32 (2001) 63–71.
- [22] P.Y. Zhang, J. Liu, *Journal of Photochemistry and Photobiology A* 167 (2004) 87–94.
- [23] V. Keller, P. Bernhardt, F. Garin, *Journal of Catalysis* 215 (2003) 129–138.
- [24] H. Einaga, S. Futamura, T. Ibusuki, *Applied Catalysis B: Environmental* 38 (2002) 215–225.
- [25] A. Bouzaza, C. Vallet, A. Laplanche, *Journal of Photochemistry and Photobiology A: Chemistry* 177 (2006) 212–217.
- [26] M.D. Hernandez-Alonso, I. Tejedor-Tejedor, J.M. Coronado, M.A. Anderson, *Applied Catalysis B: Environmental* 101 (2011) 283–293.
- [27] S.B. Kim, H.T. Hwang, S.C. Hong, *Chemosphere* 48 (2002) 437–444.
- [28] Y. Luo, D.F. Ollis, *Journal of Catalysis* 163 (1996) 1–11.
- [29] A. Maudhuit, C. Raillard, V. Hequet, L. Le Coq, J. Sablayrolles, L. Molins, *Chemical Engineering Journal* 170 (2011) 464–470.
- [30] R. Mendez-Roman, N. Cardona-Martinez, *Catalysis Today* 40 (1998) 353–365.
- [31] G. Marci, M. Addamo, V. Augugliaro, S. Coluccia, E. Garcia-Lopez, V. Loddo, G. Martra, L. Palmisano, M. Schiavello, *Journal of Photochemistry and Photobiology A* 160 (2003) 105–114.
- [32] L.X. Cao, Z. Gao, S.L. Suib, *Abstracts of Papers of the American Chemical Society* 220 (2000) 269.
- [33] S. Brosillon, L. Lhomme, C. Vallet, A. Bouzaza, D. Wolbert, *Applied Catalysis B: Environmental* 78 (2008) 232–241.
- [34] L.A. Dibble, G.B. Raupp, *Catalysis Letters* 4 (1990) 345–354.
- [35] M.L. Sauer, D.F. Ollis, *Journal of Catalysis* 158 (1996) 570–582.
- [36] J. Shang, Y.G. Du, Z.L. Xu, *Chemosphere* 46 (2002) 93–99.
- [37] V. Augugliaro, A. Bianco Prevot, J. Cáceres Vázquez, E. García-López, A. Irco, V. Loddo, S. Malato Rodríguez, G. Marci, L. Palmisano, E. Pramauro, *Advances in Environmental Research* 8 (2004) 329–335.